LAWRENCE
LIVERMORE
NATIONAL
LABORATORY

LLNL-JRNL-414580

High pressure phase transformation in iron under fast compression

M. Bastea, S. Bastea, R. Becker

July 10, 2009

Applied Physics Letters

Disclaimer

High pressure phase transformation in iron under fast compression

Marina Bastea,* Sorin Bastea, and Richard Becker

Lawrence Livermore National Laboratory,

P.O. BOX 808, Livermore, CA 94550

Abstract

We present experimental results on the solid-solid, α to ϵ phase transformation kinetics of iron under high pressure dynamic compression. We observe kinetic features - velocity loops - similar with the ones recently reported to occur when water is frozen into its ice VII phase under comparable experimental conditions. We analyze this behavior in terms of general ideas coupling the steady sample compression with phase nucleation and growth with a pressure dependent phase interface velocity. The model is used to predict the response of iron when steadily driven across the $\alpha - \epsilon$ phase boundary on very short time scales, including those envisioned to be achieved in ultra-fast laser experiments.

PACS numbers: 64.70.Dv, 64.60.Qb, 62.50.+p

*Electronic address: bastea1@llnl.gov

The transformation of a material from one stable phase to another following a change in thermodynamic conditions remains a problem of much interest both from fundamental as well as practical points of view. Well known concepts of phase nucleation and growth are being revisited and refined [1–3] due to their importance in geophysics, metallurgy, materials science [4–7] and many other fields, while new experimental techniques, particularly at high pressures, continue to open new vistas of research and exploration [8–14]. The study of phase transition kinetics under high pressures has a long history, with the earliest reported measurements being performed under static conditions by Bridgman [15]. The advent of shock wave techniques enabled probing the nature of materials' transformations under an entirely new range of experimental conditions and brought new perspectives and insights into this problem [16], dispelling for example long-held beliefs on the limits of the time scales of phase transformations in solids [17]. As new methods are being developed and new experimental regimes are being explored, fresh puzzles however continue to emerge on the behavior of materials undergoing phase transitions under conditions of very rapid compression. Recently, the quasi-isentropic uniaxial loading of liquid water across its ice VII phase boundary [18, 19] yielded dynamic features resembling Van der Waals loops, which as of yet are not fully understood from a fundamental point of view. In this paper we present fast compression experimental results on the solid - solid, α to ϵ phase transformation of iron which, surprisingly, exhibit similar characteristics with the ones observed in the liquid to solid rapid quasi-isentropic quench of water. We analyze the experimental findings using classical nucleation and growth ideas applied to steady compression conditions, clarify the physical origin of the observed dynamic features, and in addition predict the behavior of iron under a wide range of loading conditions, including those achieved in laser-driven experiments. [14].

Iron is a material of significant relevance for many research fields and applications, including the physics of the Earth's core, materials science, metallurgy, etc., and its behavior under shock conditions as well as its phase diagram at high pressures have been studied for decades [20–25]. The body-centered-cubic $Fe(\alpha)$ to hexagonal-closed-packed $Fe(\epsilon)$ phase transformation in particular has remained of interest to experimentalists and theorists alike ever since it was first reported in shock wave experiments almost fifty years ago [20]. The present ramp compression study was aimed at understanding the nature of the solid - solid transition kinetics when iron is quasi-isentropically driven, under shock-less conditions, across the α/ϵ phase boundary on time scales of the order tens to hundreds of nanoseconds. To this end,

starting from ambient, the pressure in the $Fe(\alpha)$ sample was smoothly increased by uniaxial loading over $\simeq 300ns$ up to $\simeq 35GPa$, deep into the $Fe(\epsilon)$ phase. The system evolution along different thermodynamic paths was explored by changing the initial sample temperature in the 300K to 600K range. The experiments were conducted on high purity (99.99+%) polycrystalline iron at the Sandia Z-accelerator; a sketch of the experimental set-up is shown in Fig. 1 (inset). Following an electro-magnetic pulse (see Ref. [26] for details of the pulse generation) the Al anode compresses uniaxially the iron sample. We monitored the motion of the boundary between the iron and the transparent Al_2O_3 window (henceforth designated as boundary) as the compression wave propagated through the sample - see Fig. 1, using a Doppler interferometer - VISAR [27]. The experiments were designed to achieve a high degree of uniformity in the sample loading and delay the magnetic field penetration until late stages, during pressure release. The applied pressure was independently measured during each experiment by placing a reference probe on the Al panel in the immediate vicinity of the sample. Details of the temperature control system implemented on the Z-accelerator are similar to those described in [9].

Ramp compression techniques allow the exploration of continuous thermodynamic paths, at various loading rates, and thus sample the kinetic response of the material to pressure application at conditions intermediate between room temperature isotherms and shock adiabats. Magnetic compression generators such as the Sandia Z-accelerator produce very smooth pressure profiles - $P(t)$ (see Fig. 1 - inset), which simplify the identification of phase transformation occurrences. It is well established by experiments and hydrodynamics simulations that in the absence of a phase transformation in the compressed sample its boundary velocity - $v(t)$ - follows closely the monotonic increase in the applied pressure. The thermodynamic crossing of a phase boundary on the other hand produces substantial $v(t)$ features, e.g. "plateaus" or "loops", which are not present in $P(t)$. Fig 1. shows for example representative results from independent experiments in which the initial Fe temperatures were 300K, 500K and 600K, respectively. Following the onset of pressurization the Fe/Al_2O_3 boundary starts to move with increasing acceleration until the phase transformation occurs, marked in the $v(t)$ record by a pronounced change in slope and in some cases a subsequent negative acceleration regime. A slight decrease in the boundary velocity maximum at the transition is seen as the initial sample temperature is raised, which is consistent with the negative slope of the $P(T)$ α/ϵ phase boundary in this region, see Fig. 3.

A direct test for the presence of transformation kinetics effects in the experiment is the comparison of the measured boundary velocity $v(t)$ with predictions from standard equilibrium hydrodynamic simulations. Each individual experiment was simulated using the actual experimental geometry, initial conditions and measured $P(t)$ drive. Iron was modeled using the two-phase equation of state of Ref. [28] (which reproduces accurately the α/ϵ phase boundary) , while Al and Al_2O_3 were described by well calibrated equations of state in tabular form [29]. Neither Al nor Al_2O_3 have any phase transformations in the P-T regime probed in these experiments. The simulations locate the equilibrium α/ϵ transformation at a boundary velocity of $\simeq 0.28 km/s$ for compression starting at $T_0 = 500K$, well below any signature is observed in the experimental $v(t)$ trace. We note that the pressure and temperature of the phase line crossing point as well as the associated volume change depend on the initial sample temperature. Since Fe and Al_2O_3 are closely matched in their dynamic impedance the measured boundary velocity should reflect the local occurrence of the transformation [9].

The modeling of high pressure phase transformation kinetics following very rapid compression is still in its infancy, with much effort previously focused on understanding such processes under shock conditions. Common approaches rely on simple representations of the phase transformation rates, e.g. depending linearly on the difference between the chemical potentials of the two phases [28], which reproduce some of the dynamic behavior observed in shock experiments but cannot explain more complex experimental features such as the negative acceleration loops recorded in these or the water experiments [18, 19]. We adopt here the phenomenological but physical picture proposed by Kolmogorov and others [3], where well defined domains of the growing phase increase their size at the expense of the parent phase through the motion of an infinitely thin interface. The new phase is assumed to start on either a fixed number of initial sites in the case of heterogeneous nucleation, or on sites produced at a certain well defined rate in the case of homogeneous nucleation. Since our present study concerns polycrystalline iron undergoing a solid-solid phase transformation we will focus the discussion on the heterogeneous case, which is likely dominant here. The fundamental equation of this approach is the rate of change of the volume fraction φ of the new phase: $d\varphi/dt = -\varphi^e(\varphi - \varphi_0)$ where φ_0 is the equilibrium volume fraction and φ^e is an unrestricted volume growth rate due to phase interfaces moving with a velocity u, $\varphi^e = uS$. Here S is an interface area per unit volume which in the most general case can be written

as $S \propto R(t)^{n-1}$, with $R(t)$ a typical domain size increasing as $dR/dt = u$, and n a growth dimensionality; $n = 3$ then corresponds to domains growing isotropically from point defects, while smaller exponents are due to growth from crystal edges or facets [30]. If the phase interface velocity u is assumed to be constant, as it is perhaps the case if the system, initially in the parent phase, i.e. $\varphi(t = 0) = \varphi_0 = 0$, is very suddenly quenched (by changing the temperature, pressure or both) into a thermodynamic state of pressure P and temperature T where $\varphi_0 > 0$, the above model yields a well known evolution equation for φ, which has been employed extensively to fit a variety of phenomena [3]. On the other hand more gradual quenching should take into account the dependence of the interface velocity on the changing thermodynamic conditions. The description of this process is further complicated for the present experiments by the uniaxial nature of the pressure loading. In this situation the above evolution equation needs to be coupled with hydrodynamic equations capturing the (plastic) flow of the material, thus directly modeling the sample boundary velocity measured in the experiments [19]. In the present analysis we wish to gain better insight into the physical effects contributing to such steadily driven phase transformation kinetics and focus here on a simpler scenario, where the coupling to hydrodynamics is done only in an approximate way and the process is assumed to be approximately isothermal. We consider a system in the parent phase at $t = 0$, whose density is steadily increased at a rate $d\rho/dt = \rho_0 \tau_d^{-1}$. We assume that the system is microscopically large (containing an extremely large number of atoms) but macroscopically small, with mechanical equilibrium rapidly reached within its boundaries at any prescribed density $\rho(t)$, volume fraction $\varphi(t)$ and temperature T. Such a system (which can be for example a hydrodynamical cell) is generally much larger than the phase interface thickness, and it will therefore typically contain many domains. Its pressure p at fixed $\rho(t)$, $\varphi(t)$ and T can be calculated by assuming only that the parent phase equation of state can be extrapolated into its metastable, overcompressed region, e.g. in the simplest case linearly. If the chemical potential difference between the metastable (parent) and stable (growing) phases is small, the interface velocity u is proportional with the overcompression $\Delta p = p - p_0$, $u = A\Delta p$, where p_0 is the phase transition pressure and A a prefactor; we adopt this dependence here, although more complicated forms can also be considered [31]. This approximation is for example akin with the linear dependence on undercooling typically considered for solidification from a melt following a rapid temperature quench [32]. Despite such simplifications, when taken as a whole the above considerations complicate

significantly the evolution equations for the volume fraction of the growing phase, which can now be solved only numerically.

We undertook such solutions for the material (iron) and conditions relevant for the present experiments. The initial sample density was taken to be the density of the iron sample in the α phase just as it crossed the phase boundary line, and the growing phase was the δ phase. The rate of change of the density was taken from the two-phase equilibrium hydrodynamic simulations, and it corresponds to the rightmost - see Fig. 1 - sample boundary region, whose velocity $v(t)$ was measured in the experiments. The calculations thus yield the dependence of pressure and φ on time at that boundary. These solutions exhibit an interesting and revealing feature: when the calculated pressure $p(t)$ is plotted parametrically against the density $\rho(t)$ the dependence so obtained - see Fig. 2 (inset) - is similar with that of the classical Van der Waals loops [34]. We emphasize however that, unlike an actual Van der Waals loop, which signals the existence of an equilibrium first order phase transition and requires a Maxwell construction to yield the thermodynamically consistent equation of state, this $p(t).vs.\rho(t)$ behavior is a dynamic feature which arises as a result of the interplay between steady compression and phase transformation kinetics with a pressure dependent phase interface velocity. In fact, in the limit of infinitely slow compression, i.e. very slowly varying $\rho(t)$, we recover the thermodynamically consistent two-phase equation of state, with an infinite compressibility region connecting the two phases. Moreover, the observed dynamic loops are typically well above the coexistence pressure, and the Maxwell construction does not apply here.

To directly compare with the experiments we estimated the boundary velocity $v(t)$. Since the Fe and Al_2O_3 impedances are very well matched the pressure jump across the Fe/Al_2O_3 boundary is negligible. We therefore employed the calibration of Ref. [33] for the $P - u_p$ dependence of Al_2O_3 in the elastic regime, to determine $v(t)$ from the calculated pressure $p(t)$. We show in Fig. 2 a comparison of the experimental results with our $v(t)$ solution estimates. Both the growth exponent n, and the interface velocity prefactor A are treated here as adjustable parameters. Nevertheless, the agreement with the experimental behavior is remarkable, both for the size and position of the velocity loop. For the majority of the samples we find $n \simeq 2$, corresponding to heterogeneous nucleation initiated mostly on crystal edges [30]. The motion of solid-solid interfaces is usually assumed to be controlled by an energy barrier limiting the movement of an atom across an interface [35]. We test the

validity of this assumption for the α to ϵ Fe transformation by analyzing the dependence of the interface velocity prefactor A on temperature. We find that an Arrhenius dependence holds quite well, with a barrier of $\simeq 285K$.

The evolution of the system becomes dominated by the phase transition kinetics at an $\epsilon - Fe$ volume fraction of $\simeq 0.13$ (close to the percolation threshold), signaled by the local maximum of $v(t)$ and a corresponding pressure $P_{eq} + \delta P_{max}$; the transformation continues to accelerate and completes at $P_{eq} + \delta P_f$. The overcompressions at the onset and completion of the transformation have been calculated from fits of the above model to the experimental data, and are shown in Fig. 3 in relationship to the $\alpha - \epsilon$ phase line. In $P(\rho)$ space, the trajectory of the Fe sample deviates from the initial α compression isentrope past the onset overpressure δP_0 and ultimately merges into an ϵ isentrope upon completion of the transformation. Since ramp compression experiments can be conducted on timescales ranging from tens to thousands of nanoseconds we also computed the projected response to a range of drives, τ_d, and the results are shown in Fig. 4. The completion times τ_c for the transformation exhibit an approximate power-law dependence on the drive τ_d - Fig. 4(inset), with an exponent of $\alpha \simeq 3/4$. The velocity loops become broader and shallower at slower compressions, e.g. those typical for gas-gun drivers [36]. On faster time-scales, such as those achieved with lasers, the loops are predicted to form at higher velocities and then eventually disappear - see Fig. 4. This is a consequence of the transformation kinetics being strongly overdriven and the transition completing at significantly higher δP_f, after sampling deeper through the non-equilibrium regime. For such experiments however the samples are necessarily much thinner and may have a larger density of initial nucleating "defects"; one such example is shown in Fig. 4 (dashed line). Finally, we note that in the limit of very fast compression it is possible and quite likely that phases occupying only a small thermodynamic region of stability may become kinetically inhibited and be actually "skipped" over. For a possible such scenario see [14].

In sum, we present experimental results on the solid-solid, α to ϵ phase transformation kinetics of iron under fast compression. We observe kinetic features - velocity loops - similar with the ones occurring when water is frozen into its ice VII phase under comparable experimental conditions. We model this behavior in terms of general phase nucleation and growth ideas coupling the steady sample compression to phase transformation kinetics with a pressure dependent phase interface velocity. These concepts can also be employed to pre-

dict the behavior of materials steadily driven across a phase boundary on very short time scales, including those envisioned to be achieved in laser experiments.

We thank the technical staff at the Sandia Z-accelerator for assistance in executing the experiments. This work was performed under the auspices of the U. S. Department of Energy by Lawrence Livermore National Laboratory under Contract DE-AC52-07NA27344.

---

[1] E.A. Brener, S.V. Iordanski, V.I. Marchenko, Phys. Rev. Lett. **82**, 1506 (1999).

[2] L. Zhang, L.-Q. Chen, Q. Du, Phys. Rev. Lett. **98**, 265703 (2007).

[3] B.A. Berg, S. Dubey, Phys. Rev. Lett. **100**, 165702 (2008) and references therein.

[4] V.S. Solomatov, D.J. Stevenson, Earth Planet. Sci. Lett. **125**, 267 (1994).

[5] E.J. Mittemeijer, J. Mat. Sci. **27**, 3977 (1992).

[6] T. Okada, W. Utsumi, H. Kaneko, V. Turkevich, N. Hamaya, and O. Shimomura, Phys. Chem. Minerals **31**, 261 (2004).

[7] J.-i. Jang, M.J. Lance, S. Wen, T.Y. Tsui, G.M. Pharr, Acta Materialia **53**, 1759 (2005).

[8] K. Jacobs, D. Zaziski, E.C. Scher, A.B. Herhold, A.P. Alivisatos, Science **293**, 1802 (2001).

[9] M. Bastea, S. Bastea, J.A. Emig, P.T. Springer, D.B. Reisman, Phys. Rev. B **71**, 180101 (2005).

[10] M. Ross, R. Boehler, D. Erradonea Phys. Rev. B **76**, 184117 (2007).

[11] B. Yaakobi et al Phys. Rev. Lett. **95**, 075501 (2005).

[12] D. KAlantar et al Phys. Rev. Lett. **95**, 075502 (2005).

[13] M. Bastea, D.B. Reisman, App. Phys. Lett. **90**, 171921 (2007).

[14] R.F. Smith, J.H. Eggert, M.D. Saculla, A.F. Jankowski, M. Bastea, D. G. Hicks, G. W. Collins, Phys. Rev. Lett. **101**, 065701 (2008).

[15] P.W. Bridgman, Proc. Am. Acad. Arts Sci **52**, 57 (1916).

[16] G.E. Duvall, R.A. Graham, Rev. Mod. Phys. **49**, 523 (1977) and references therein.

[17] P.W. Bridgman, J. Appl. Phys. **27**, 659 (1956).

[18] D.H. Dolan, M.D. Knudson, C.A. Hall, C. Deeney, Nature Phys. **3**, 339 (2007).

[19] M. Bastea, S. Bastea, J.E. Reaugh, D.B. Reisman, Phys. Rev. B **75**, 172104 (2007).

[20] R.E. Duff, S. Minshall, Phys. Rev. **108**, 1207 (1957).

[21] A. Papandrew et al, Phys. Rev. B **69**, 144301 (2004).

[22] A. Dewaele, M. Torrent, P. Loubeyre, M. Mezouar, Phys. Rev. B **78**, 104102 (2008).

[23] T. de Resseguier, M. Hallouin, Phys. Rev. B **77**, 174107 (2008).

[24] K. Kadau, T.C. Germann, P.S. Lomdahl, B.L. Holian, Phys. Rev. B **72**, 064120 (2005).

[25] A.B. Belonoshko et al, Phys. Rev. B **78**, 104107 (2008).

[26] C.A. Hall, J.R. Asay, M.D. Knudson, W.A. Stygar, R.B. Spielman, T.D. Pointon, D.B. Reisman, A. Toor, R.C. Cauble, Rev. Sci. Instr. **72**, 3587 (2001).

[27] Hemsing, Rev. Sci. Instr. **50** 73(1979); L.M.Barker *Shock Compression of Condensed Matter - 1997* edited by S.C. Schmidt, D.P.Dandekar and J.W.Forbes (American Institute of Physics, Woodbury, NY, 1998), pp.833-6.

[28] J. C. Boettger and D. C. Wallace, Phys. Rev. B **55**, 2840 (1997).

[29] D.A.Young and E.M. Corey, J. Appl Phys **78**, 3748 (1995).

[30] J.M. Cahn, Acta Metall. **4**, 449 (1956).

[31] N. Hamaya, Y. Yamada, J.D. Axe, D.P. Belanger, S.M. Shapiro, Phys. Rev. B **33**, 7770 (1986).

[32] M. Amini, B.B. Laird, Phys. Rev. Lett. **97**, 216102 (2006).

[33] O.V. Fat'yanov, R.L. Webb and Y. Gupta, J. Appl. Phys. **97**, 123539 (2005).

[34] See, e.g., M.E. Fisher, S. Zinn, J. Phys. A **31**, 629 (1998) and references therein.

[35] D. Turnbull, in *Solid State Physics*, edited by F. Seitz and D. Turnbull (Academic, London, 1956), Vol. 3, p. 225.

[36] J. Nguyen, D. Orlikowski, F. Streitz, N. Holmes, J. Moriarty AIP Conf. Proc. **706**, 1225 (2004).

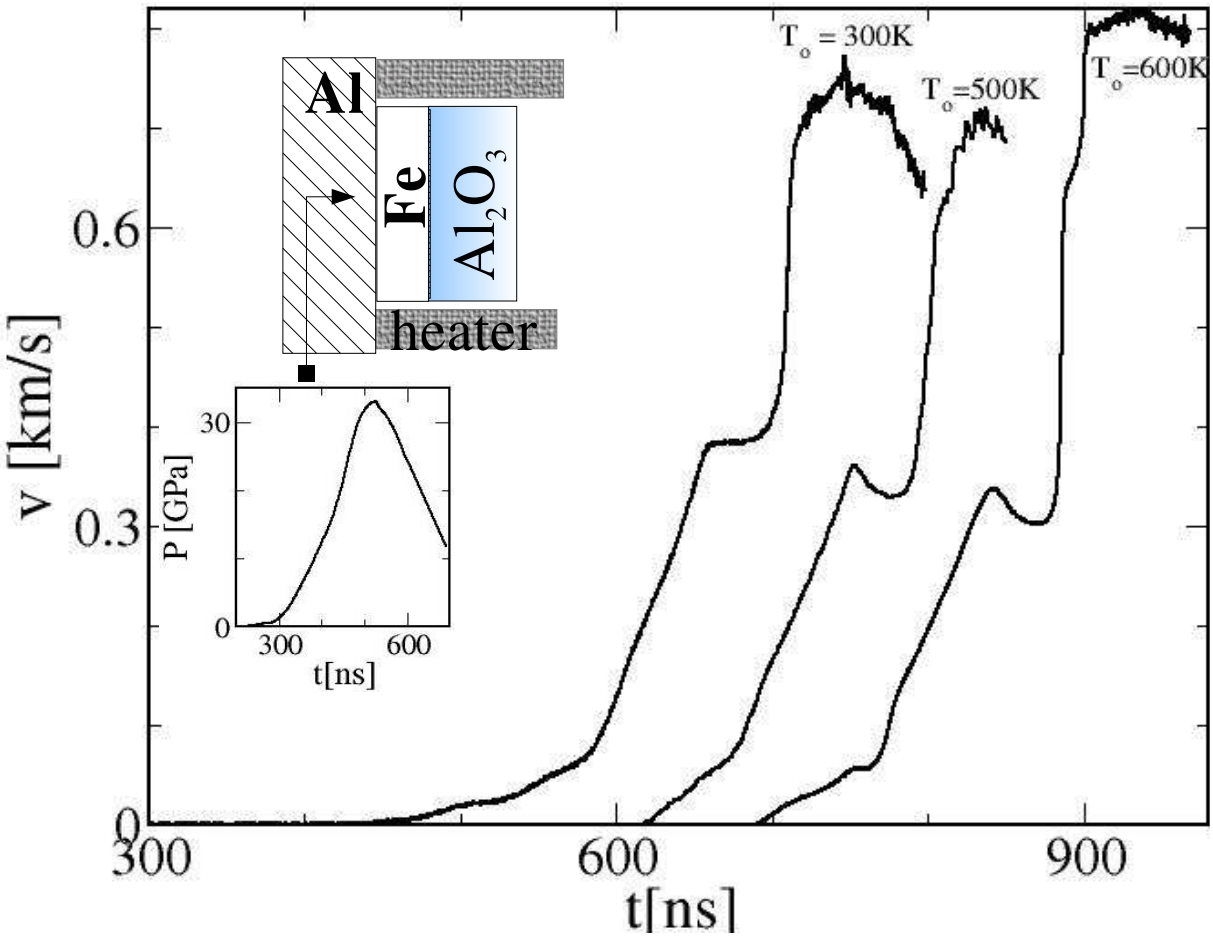

FIG. 1: Measured Fe/Al_2O_3 boundary velocity history, for several initial sample temperatures ; sliding time scale. Inset: Sketch of the experimental geometry including the Al anode, Fe sample, Al_2O_3 window and the heater block. $P(t)$ is the measured driving pressure at the Al/Fe boundary.

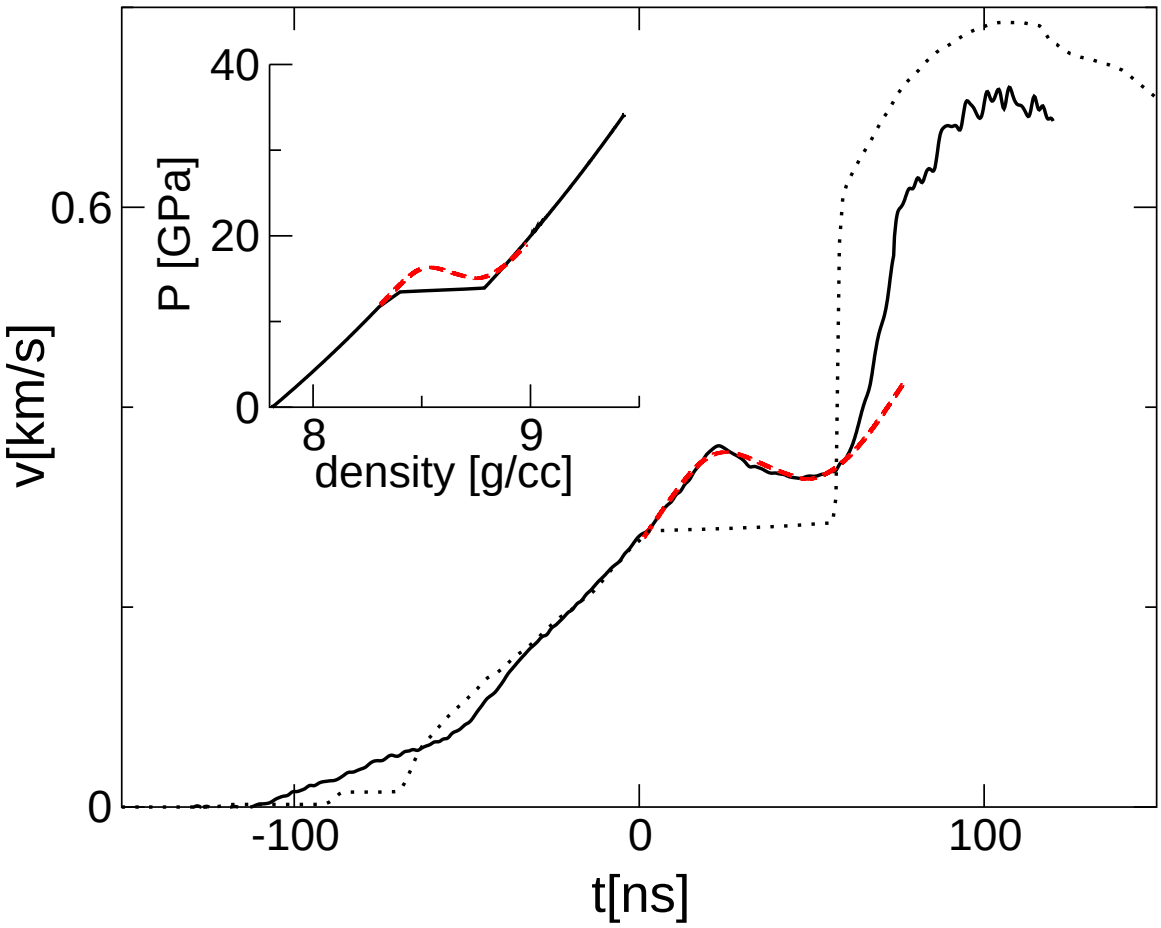

FIG. 2: Experimental data, equilibrium hydrodynamic simulations and kinetics model in black solid, black dotted and red dashed lines, respectively. Inset: Parametric plot of the pressure.vs. density for Fe according to equilibrium simulations - black solid, and kinetics model - red dashed.

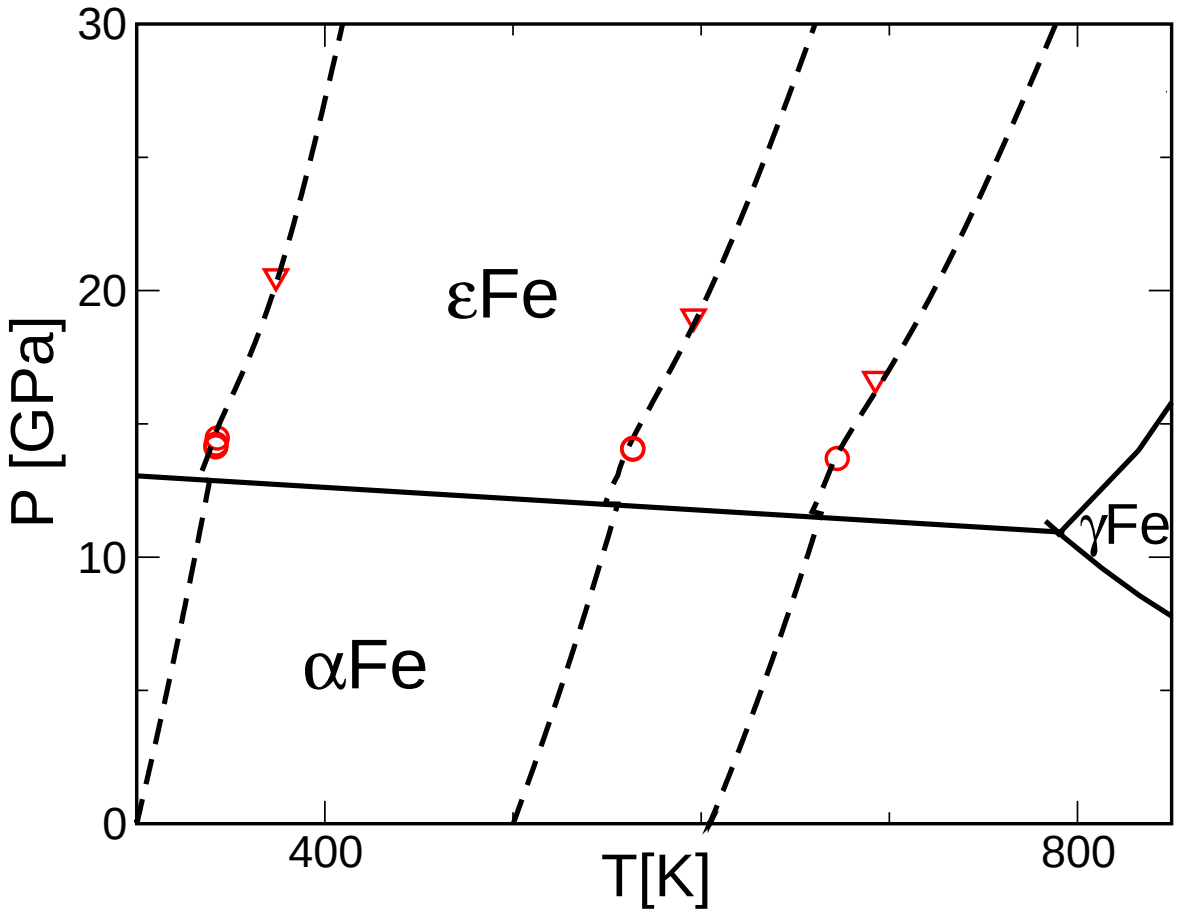

FIG. 3: Phase diagram of Fe and phase space trajectories (dashed lines) explored in the experiments. The onset and completion of the α/ϵ transition according to the kinetics model are marked by red circles and triangles, respectively.

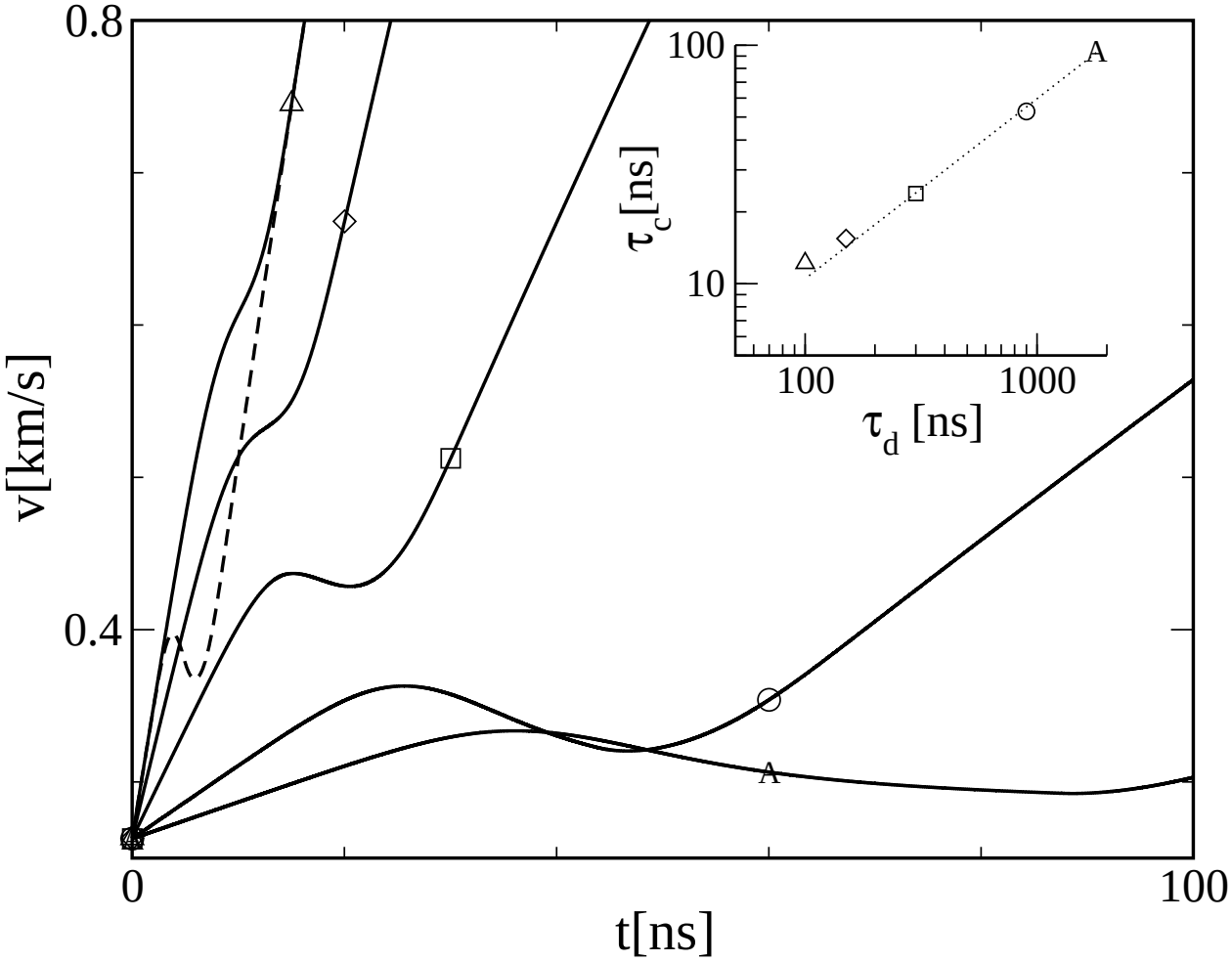

FIG. 4: Projected sample response at various driving conditions along with the corresponding completion time for the phase transition (inset).